Inorg. Chem. **2006**, *45*, 5996–6003

Synthesis, Characterization, and Electrochemistry of Diruthenium(III,II) and Monoruthenium(III) Complexes Containing Pyridyl-Substituted 2-Anilinopyridinate Ligands

Karl M. Kadish,*,† Minh Nguyen,† Eric Van Caemelbecke,†,‡ and John L. Bear*,†

Department of Chemistry, University of Houston, Houston, Texas 77204-5003, and Houston Baptist University, 7502 Fondren Road, Houston, Texas 77074-3298

Received February 15, 2006

Reaction of the metal–metal bonded complex $Ru_2(O_2CCH_3)_4Cl$ with 2-anilino-4-methylpyridine leads to the (3,1) isomer of the diruthenium(III,II) complex $Ru_2(ap\text{-}4\text{-}Me)_4Cl$, **1** while the same reaction with 2-anilino-6-methylpyridine gives the monoruthenium(III) derivative $Ru(ap\text{-}6\text{-}Me)_3$, **2**. Both compounds were examined as to their structural, electrochemical, and UV–visible properties, and the data were then compared to that previously reported for (4,0) $Ru_2(2\text{-}Meap)_4Cl$ and other (3,1) isomers of $Ru_2(L)_4Cl$ with similar anionic bridging ligands. ESR spectroscopy indicates that the monoruthenium derivative **2** contains low-spin Ru(III), and the presence of a single ruthenium atom is confirmed by an X-ray structure of the compound. The combined electrochemical and UV–vis spectroelectrochemical data indicate that the diruthenium complex **1** is easily converted to its Ru_2^{4+} and Ru_2^{6+} forms upon reduction or oxidation by one electron while the monoruthenium derivative **2** also undergoes metal-centered redox processes to give Ru^{II} and Ru^{IV} complexes under the same solution conditions. The reactivity of **1** with CO and CN^- was also examined.

Introduction

Our laboratory[1−16] and others[17−26] have previously synthesized a variety of diruthenium and dirhodium complexes of the type $[Ru_2(L)_4]^n$ or $[Rh_2(L)_4]^n$ where $n = 0$, $+1$, or $+2$ and L is 2-anilinopyridinate (ap) or substituted ap bearing electron-withdrawing or electron-donating groups at the ortho, meta, or para position on the anilino site of the ap ligand. Although four different isomeric forms of the metal−metal-bonded compounds are theoretically possible,[4,6,11,13−15] the majority of characterized diruthenium or dirhodium

* To whom correspondence should be addressed. E-mail: kkadish@uh.edu (K.M.K.), jbear@uh.edu (J.L.B.).

† University of Houston.

‡ Houston Baptist University.

(1) Bear, J. L.; Han, B.; Huang, S.; Kadish, K. M. *Inorg. Chem.* **1996**, *35*, 3012−3021.
(2) Bear, J. L.; Li, Y.; Han, B.; Kadish, K. M. *Inorg. Chem.* **1996**, *35*, 5, 1395−1398.
(3) Bear, J. L.; Li, Y.; Han, B.; Van Caemelbecke, E.; Kadish, K. M. *Inorg. Chem.* **1996**, *35*, 3053−3055.
(4) Bear, J. L.; Li, Y.; Han, B.; Van Caemelbecke, E.; Kadish, K. M. *Inorg. Chem.* **1997**, *36*, 5449−5456.
(5) Bear, J. L.; Li, Y.; Han, B.; Van Caemelbecke, E.; Kadish, K. M. *Inorg. Chem.* **2001**, *40*, 182−186.
(6) Bear, J. L.; Wellhoff, J.; Royal, G.; Van Caemelbecke, E.; Eapen, S.; Kadish, K. M. *Inorg. Chem.* **2001**, *40*, 2282−2286.
(7) Bear, J. L.; Yao, C. L.; Liu, L. M.; Capdevielle, F. J.; Korp, J. D.; Albright, T. A.; Kang, S. K.; Kadish, K. M. *Inorg. Chem.* **1989**, *28*, 1254−1262.
(8) Bear, J. L.; Yulan, L.; Jing, C.; Boacheng, H.; Van Caemelbecke, E.; Phan, T. D.; Kadish, K. M. *Inorg. Chem.* **2000**, *39*, 857−861.
(9) Bear, J. L.; Wu, B. H. Z.; Van Caemelbecke, E.; Kadish, K. M. *Inorg. Chem.* **2001**, *40*, 2275−2281.
(10) Bear, J. L.; Chen, W.-Z.; Han, Boacheng; Huang, S.; Wang, Li-Lun; Thuriere, A.; Van Caemelbecke, E.; Kadish, K. M.; Ren, T. *Inorg. Chem.* **2003**, *42*, 6230−6240.
(11) Kadish, K.; Wang, L.-L.; Thuriere, A.; Giribabu, L.; Garcia, R.; Van Caemelbecke, E.; Bear, J. L. *Inorg. Chem.* **2003**, *42*, 8309−8319.
(12) Kadish, K. M.; Boacheng, H.; Shao, J.; Ou, Z.; Bear, J. L. *Inorg. Chem.* **2001**, *40*, 6848−6851.
(13) Kadish, K. M.; Wang, L.-L.; Thuriere, A.; Van Caemelbecke, E.; Bear, J. L. *Inorg. Chem.* **2003**, *42*, 834−843.
(14) Kadish, K. M.; Phan, T. D.; Giribabu, L.; Van Caemelbecke, E.; Bear, J. L. *Inorg. Chem.* **2003**, *42*, 8663−8673.
(15) Kadish, K. M.; Phan, T. D.; Giribabu, L.; Shao, Jianguo; Wang, Li-Lun; Thuriere, Antoine; Van Caemelbecke, Eric; Bear, J. L. *Inorg. Chem.* **2004**, *43*, 1012−1020.
(16) Kadish, K. M.; Phan, T. D.; Giribabu, L.; Shao, Jianguo; Wang, Li-Lun; Thuriere, Antoine; Wellhoff, J.; Van Caemelbecke, Eric; Bear, J. L. *Inorg. Chem.* **2004**, *43*, 4825−4832.
(17) Chakravarty, A. R.; Cotton, F. A. *Inorg. Chim. Acta* **1986**, *113*, 19−26.
(18) Chakravarty, A. R.; Cotton, F. A.; Tocher, D. A. *Inorg. Chem.* **1985**, *24*, 172−177.
(19) Cotton, F. A.; Yokochi, A. *Inorg. Chem.* **1997**, *36*, 567−570.
(20) Ren, T. *Organometallics* **2005**, *24*, 4854−4870.
(21) Ren, T.; Zou, G.; Alvarez, J. C. *Chem. Commun.* **2000**, 1197−1198.
(22) Shi, Y.; Yee, G. T.; Wang, G.; Ren, T. *J. Am. Chem. Soc.* **2004**, *126*, 10552−10553.

10.1021/ic060267k CCC: $33.50
Published on Web 06/20/2006

Chart 1. Position of Methyl (R) Substituent on the ap Ligand

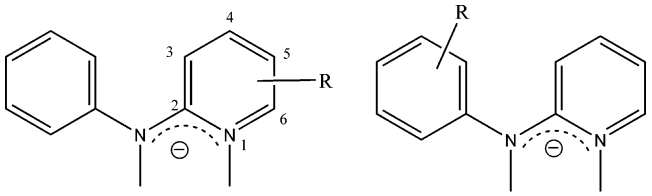

a) pyridyl substitution. b) anilino substitution.

derivatives have been isolated either in a single isomeric form or as a mixture of only two isomers, labeled as the (3,1) and (4,0) isomers.

The percent yield for synthesis of a given isomer of $Ru_2(L)_4Cl$ or $Rh_2(L)_4Cl$ was shown in recent studies from our laboratory to vary between 0% and 73% for the (4,0) isomer and between 0% and 53% for the (3,1) isomer, but there was no obvious trend with either the number of substituents on the ap bridging ligand or the electronic effects of these substituents.[6,13] There was also no evident trend between the number and type of isomers in the reaction product and the position of substituents on the anilino part of the ligand, i.e., ortho, meta, or para. We therefore wished to know if the isomeric distribution might become predictable if the substituents were added not to the anilino but rather to the pyridyl part of the ap ligand, and this is investigated in the present paper.

We were especially interested in generating diruthenium compounds with bridging ap ligands having ortho-substituted pyridyl groups (Chart 1a) since a great deal is known about the analogous diruthenium or dirhodium complexes where substitution is at the ortho part of the anilino group (Chart 1b).[4−6,8,10,11,13−16,27]

We were readily able to synthesize the pyridyl-substituted compound, $Ru_2(ap\text{-}4\text{-}Me)_4Cl$, **1**, which was characterized as exclusively the (3,1) isomer, but surprisingly, all attempts to generate a diruthenium complex with a methyl substituent on the ortho (ap-6-Me) position of the pyridyl group failed and only a neutral monoruthenium complex, characterized as $Ru(ap\text{-}6\text{-}Me)_3$, **2**, was obtained. Although neutral $Ru(L)_3$ complexes are known,[28−33] the unexpected synthesis of **2** provided us with the opportunity to directly compare the behavior of monoruthenium and diruthenium derivatives with similar pyridyl-substituted ap ligands under the same experimental conditions, thus giving information on how similar anionic ligands will affect the redox properties and UV−vis spectra of Ru^{2+}, Ru^{3+}, and Ru^{4+} as opposed to Ru_2^{4+}, Ru_2^{5+}, and Ru_2^{6+}. The structural properties of both compounds **1** and **2** in their neutral form are reported in the present paper, and the data for **1** are compared to (4,0) $Ru_2(2\text{-}Meap)_4Cl$[13] and previously characterized (3,1) isomers of other $Ru_2(L)_4Cl$ complexes having ap bridging ligands with substitution on the anilino part of the molecule.[6,11,13−15]

Experimental Section

Chemicals and Reagents. Ultrahigh purity nitrogen and CO gases were purchased from Matheson−Trigas and used as received. GR graded dichloromethane, hexanes, acetones, and absolute dichloromethane (for electrochemistry and UV−vis spectroscopy) were all purchased from EMD or Aldrich and were used without further purification. Benzonitrile (PhCN) was also purchased from Aldrich and was distilled over P_2O_5 prior to use. Tetra-*n*-butylammonium perchlorate (TBAP) and tetra-*n*-butylammonium cyanide (TBACN) were obtained from Fluka, recrystallized from ethyl alcohol, and stored in a vacuum oven at 40 °C for at least 2 weeks prior to use. 2-Bromo-*X*-methyl pyridine (C_6H_6BrN) where $X = 4$ or 6, aniline (C_6H_7N), lithium chloride (LiCl), ruthenium chloride hydrate ($RuCl_3 \cdot 3H_2O$), silica gel (Merck 230−400 mesh 60 Å), and $CDCl_3$ (99.8% atom in D, for NMR measurements) were purchased from Aldrich and used as received.

Physical Measurements. Cyclic voltammetry was carried out with an EG&G model 263A potentiostat/galvanostat. A three-electrode system was used and consisted of a glassy carbon or platinum disk working electrode, a platinum wire counter electrode, and a homemade saturated calomel electrode (SCE) as the reference electrode. The SCE was separated from the bulk of the solution by a fritted-glass bridge of low porosity containing the solvent/supporting electrolyte mixture. All potentials are referenced to the SCE, and measurements were carried out at room temperature or at low temperature (about −70 °C) by inserting the electrochemical cell into a slush bath containing a mixture of acetone and dry ice. UV−visible spectroelectrochemistry experiments were carried out with a Hewlett-Packard Model 8453 diode-array spectrophotometer.

^{1}H NMR measurements were recorded at room temperature on a General Electric QE-300 Plus spectrometer and were referenced to tetramethylsilane (TMS). ESR spectra were recorded on a Bruker ER 100E spectrometer. The *g* values were measured with respect to diphenylpicrylhydrazyl (DPPH: $g = 2.0036 \pm 0.0003$). Magnetic susceptibilities were measured according to the Evans method[34] on a General Electric QE-300 FT NMR spectrometer in $CDCl_3$ with TMS as the internal reference compound. Mass spectra were recorded on an Applied Biosystem Voyager DE-STR MALDI-TOF mass spectrometer equipped with a nitrogen laser (337 nm) at the University of Houston Mass Spectrometry Laboratory.

Synthesis of 2-Anilino-*X*-methylpyridine ($X = 4$ or 6). The appropriate freshly distilled aniline (7.00 mL, 76.8 mmol) and 2-bromo-6-methyl pyridine (2.5 mL, 21.9 mmol) were added to a dried and N_2-flushed 50 mL round-bottom flask equipped with a condenser and a magnetic stirring bar. The mixture was heated to 170 °C and left to react overnight. 10% NaOH (20 mL) was then added to the flask, and the mixture stirred for 15 min. The contents of the flask were transferred into a 250 mL round-bottom flask, which was filled with water, after which it was steam distilled until

(23) Xu, G.; Ren, T. *Organometallics* **2001**, *20*, 2400−2404.
(24) Xu, G.; Ren, T. *Inorg. Chem.* **2001**, *40*, 2925−2927.
(25) Xu, G.-L.; Wang, C.-Y.; Ni, Y.-H.; Goodson, T. G., III; Ren, T. *Organometallics* **2005**, *24*, 3247−3254.
(26) Zhang, L.-Y.; Chen, J.-L.; Shi, L.-X.; Chen, Z.-N. *Organometallics* **2002**, *21*, 5919−5925.
(27) Nakanishi, T.; Thuriere, A.; Bear, J. L.; Kadish, K. M. *Electrochem. Solid-State Lett.* **2004**, *7*, E6−E9.
(28) Bardwell, D. A.; Black, D.; Jeffery, J. C.; Schatz, E.; Ward, M. D. *J. Chem. Soc., Dalton Trans* **1993**, 2321−2327.
(29) Bennett, M. A.; Heath, G. A.; Hockless, D. C. R.; Kovacik, I.; Willis, A. C. *Organometallics* **1998**, *17*, 5867−5873.
(30) Das, A.; Peng, S.-M.; Lee, G.-H.; Bhattacharya, S. *New J. Chem.* **2004**, *28*, 712−717.
(31) Frey, G. D.; Bell, Z. R.; Jeffery, J. C.; Ward, M. D. *Polyhedron* **2001**, 3231−3237.
(32) Singh, A. K.; Balamurugan, V.; Mukkherjee, R. *Inorg. Chem.* **2003**, *42*, 6497−6502.
(33) Thompson, A. M. W. C.; Bardwell, D. A.; Jeffery, J. C.; Rees, H.; Ward, M. D. *J. Chem. Soc., Dalton Trans* **1997**, 721−726.
(34) Evans, J. *J. Chem. Soc.* **1959**, 2003−2005.

about 75 mL of distillate was obtained and discarded. The residue left in the round-bottom flask was collected and extracted with CH_2Cl_2 (3 × 50 mL). The organic phases were combined and dried with $MgSO_4$. The solvent was removed with a rotary evaporator. For L = ap-4-Me, the residue obtained after evaporation was recrystallized with acetone/hexanes (1:20, v/v) to afford white crystals with a 95% yield. For L = ap-6-Me, the residue after evaporation of the solvent was further distilled and the title product recovered as a white oil in an 85% yield. L = ap-4-Me: mass spectral data [*m*/*e*, (fragment)]: 185.4 [Hap-6-Me]$^+$. ^{1}H NMR (in $CDCl_3$): 8.10 (s, 1H), 7.34 (m, 5H), 7.07 (m, 1H), 6.60 (d, 1H), 6.53 (s, 1H), 2.30 (s, 3H) ppm. ^{13}C NMR (in $CDCl_3$): 154.6, 148.5, 141.7, 139.1, 129.8, 124.5, 123.1, 122.7, 120.3, 108.7, 18.1. L = ap-6-Me: mass spectral data [*m*/*e*, (fragment)]: 185.4 [Hap-6-Me]$^+$. ^{1}H NMR (in $CDCl_3$): 7.41 (m, 3H), 7.22 (t, 2H), 6.87 (t, 1H), 6.79 (dd, 2H), 3.22 (s, 1H), 2.31 (s, 3H) ppm. ^{13}C NMR (in $CDCl_3$): 157.9, 156.1, 141.3, 138.5, 129.8, 123.1, 123.0, 120.8, 114.9, 105.3, 24.8 ppm.

Synthesis of 1. The synthesis of the title compound was carrying out using two different methods, giving in each case **1** after purification. However, the first method using a melt rather than solution gave consistently higher yields.

Method 1. $Ru_2(O_2CCH_3)_4Cl$[35,36] (0.08 g, 0.173 mmol) and H(ap-4-Me) (1.02 g, 5.54 mmol) were added to a 25 mL round-bottom flask. The mixture was stirred and flushed with N_2 for 15 min prior to heating to 110 °C under vacuum for 3 h. The crude product was then sublimed at 110 °C in order to remove excess ligand. The residue was purified on a silica gel column using acetone/hexanes (3:7, v/v); only a single green band was observed. The solvent was removed to afford green crystals of (3,1) $Ru_2(L)_4Cl$ in a 52% yield.

Method 2. $Ru_2(O_2CCH_3)_4Cl$[35,36] (0.10 g, 0.215 mmol) and H(ap-4-Me) (1.26 g, 6.88 mmol) were added to a 25 mL round-bottom flask. The mixture was stirred and flushed with nitrogen for 15 min prior to adding toluene (10 mL) and refluxing under nitrogen for 20 h. The reaction mixture was filtered to remove unreacted $Ru_2(O_2CCH_3)_4Cl$, the filtrate collected, and the solvent evaporated under vacuum. The crude product was sublimed at 110 °C under vacuum to removed excess ligand. The residue was purified by silica gel column chromatography using acetone/hexanes (3:7, v/v) as eluent; only a single green band was observed. The title compound was recovered as green crystals in a 22% yield (R_f = 0.45). UV−vis spectrum of **1** in CH_2Cl_2 [λ_{max}, nm ($\epsilon \times 10^{-3}$, M^{-1} cm^{-1})]: 331 (8.9), 431 (2.3), 467 (2.1), 732 (2.6). Mass spectral data [*m*/*e*, (fragment)]: 936 [Ru_2(ap-4-Me)$_4$]$^+$, 971 [Ru_2(ap-4-Me)$_4$-Cl]. Anal. Calcd for $C_{48}H_{44}ClN_8Ru_2$·0.5acetone: C, 59.84; H, 4.74; N, 11.21. Found: C, 60.07; H, 4.81; N, 11.29. Magnetic moment: 4.19 μ_B at 297 K.

Synthesis of 2. Two methods were also used to synthesize this compound, and both gave the same title compound after purification. Again, the first method using a melt rather than solution gave consistently higher yields.

Method 1. $Ru_2(O_2CCH_3)_4Cl$[35,36] (0.11 g, 0.236 mmol) and H(ap-6-Me) (1.39 g, 7.55 mmol) were added to a 25 mL round-bottom flask. The mixture was stirred and flushed with nitrogen for 15 min then heated to 110 °C under vacuum for 5 h. The crude product was then distilled at 110 °C under vacuum to remove excess ligand. The residue was then purified on a silica gel column using an acetone/hexanes (3:7, v/v) mixture as eluent, and green crystals of the title compound were recovered in a 70% yield.

(35) Stephenson, T. A.; Wilkinson, G. *J. Inorg. Nucl. Chem.* **1966**, *28*, 2285.
(36) Mitchell, R. W.; Spencer, A.; Wilkinson, G. *J. Chem. Soc., Dalton Trans* **1973**, 846.

Table 1. Crystal Data and Data Collection and Processing Parameters for **1** and **2**

	1	**2**
mol. formula	$C_{54}H_{56}N_8O_2ClRu_2$	$C_{36}H_{33}N_6Ru$
fw (g/mol)	1086.66	650.75
space group	$P2_1/n$ monoclinic	$P1$ triclinic
a (Å)	10.8481(6)	9.7954(4)
b (Å)	25.2854(15)	12.7306(5)
c (Å)	18.7165(11)	13.0719(6)
α (deg)	90	81.534(1)
β (deg)	101.805(1)	75.846(1)
γ (deg)	90	79.352(1)
V (Å^3)	5025.3(5)	1544.45(11)
Z	4	2
ρ_{calcd} (g/cm^3)	1.436	1.399
μ (mm^{-1})	0.703	0.543
λ (Mo Kα) (Å)	0.71073	0.71073
temp (K)	223	223
final R indices [$I > 4\sigma(I)$]	R1 = 0.0190	R1 = 0.0356
	wR2 = 0.0491	wR2 = 0.0893
R indices (all data)	R1 = 0.0209	R1 = 0.0657
	wR2 = 0.0506	wR2 = 0.1139

Method 2. $Ru_2(O_2CCH_3)_4Cl$[35,36] (0.10 g, 0.215 mmol) and H(ap-6-Me) (1.26 g, 6.88 mmol) were added to a 25 mL round-bottom flask. The mixture was stirred and flushed with nitrogen for 15 min after which toluene (10 mL) was added and the mixture was again refluxed under nitrogen for 20 h. The reaction mixture was filtered to remove unreacted $Ru_2(O_2CCH_3)_4Cl$ after which the filtrate was collected and the solvent evaporated under vacuum. The crude product was distilled at 110 °C under vacuum in order to remove excess ligand. The residue was eluted on a silica gel column using an acetone/hexanes (3:7, v/v) mixture, and green crystals of the title compound were recovered in a 40% yield (R_f = 0.50). UV−vis spectrum in CH_2Cl_2 [λ_{max}, nm ($\epsilon \times 10^{-3}$, M^{-1} cm^{-1})]: 310 (32), 750 (3.5). Mass spectral data [*m*/*e*, (fragment)]: 651 [Ru(ap-6-Me)$_3$]. Anal. Calcd for $C_{36}H_{33}N_6Ru$: C, 66.44; H, 5.11; N, 12.91. Found: C, 66.69; H, 5.28; N, 12.91. Magnetic moment: 1.75 μ_B at 297 K.

X-ray Crystallography of 1 and 2. Single-crystal X-ray crystallographic studies were performed at the University of Houston X-ray Crystallographic Center. Each sample was placed in a stream of dry nitrogen gas at −50 °C in a random position. The radiation used was Mo Kα monochromatized by a highly ordered graphite crystal. Final cell constants and other information pertinent to data collection and structure refinement are listed in Table 1. All measurements were made with a Siemens SMART platform diffractometer equipped with a 1K CCD area detector. A hemisphere of data 1271 frames at 5 cm detector distance was collected using a narrow-frame method with scan widths of 0.30° ω and an exposure time of 30 s/frame. The first 50 frames were measured again at the end of data collection to monitor instrument and crystal stability, and the maximum correction on I was <1%. The data were integrated using the Siemens SAINT program, with the intensities corrected for Lorentz factor, polarization, air absorption, and absorption due to variation in the path length through the dectector faceplate. A ψ-scan absorption correction was applied on the basis of the entire data set. Redundant reflections were averaged.

Results and Discussion

Structural Characterization of 1. An ORTEP diagram of **1** is shown in Figure 1, while selected bond lengths and bond angles are given in Table 2 which also includes selected bond lengths and bond angles of Ru_2(2-Meap)$_4Cl$ for

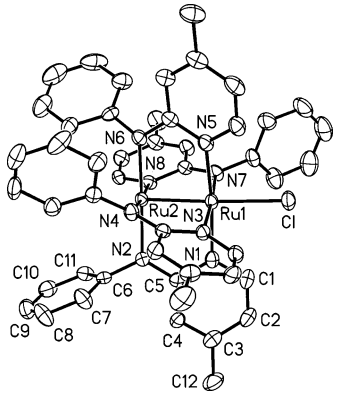

Figure 1. Molecular structure of (3,1) Ru_2(ap-4-Me)$_4$Cl, **1**. H atoms have been omitted for clarity.

Table 2. Selected Bond Lengths (Å) and Bond Angles (deg) for **1** and Ru_2(2-Meap)$_4$Cl[a]

	1	Ru_2(2-Meap)$_4$Cl
	Bond Lengths (Å)	
Ru−Ru	2.2906(6)	2.279
Ru−Cl	2.4770(13)	2.487
Ru−N_p[b]	2.095	2.101
Ru−N_a[c]	2.044	2.053
	Bond Angles (deg)	
Ru−Ru−Cl	177.64(4)	180.0
Ru−Ru−N_a	89.8	89.5
Ru−Ru−N_p	89.2	87.8
N−Ru−Ru−N	13.9	21.6

[a] See ref 1. [b] N_p, pyridyl nitrogen. [c] N_a, anilino nitrogen.

comparison purposes. The coordination of Ru1 and Ru2 in **1** is octahedral and square pyramidal, respectively, and the four "ap-4-Me" ligands form the equatorial plane of the diruthenium complex. The Ru1 atom is coordinated to one Cl^- axial ligand, three pyridyl nitrogen atoms, and one anilino nitrogen atom while the Ru2 atom is coordinated to three anilino nitrogen atoms and one pyridyl nitrogen atom. Therefore, the Cl^- axial ligand is bound to the ruthenium atom coordinated with three pyridyl groups and this was also the case for the (3,1) isomers of Ru_2(2-Fap)$_4$Cl, Ru_2(2,6-F_2-ap)$_4$Cl, and Ru_2(2,4,6-F_3ap)$_4$Cl.[13]

The Ru−Ru bond length of **1** is 2.2906(6) Å, and this value is within the range of Ru−Ru bond lengths for other (3,1) and (4,0) diruthenium complexes with four identical "ap-type" ligands (2.275−2.296 Å).[13] The Ru−Cl bond distance of compound **1** is 2.4770(13) Å, and this value is also in the range of Ru−Cl bond lengths for (3,1) and (4,0) isomers of Ru_2(Xap)$_4$Cl (2.437−2.487 Å) where X is a substituent on the anilino part of the ap ligand.[13] The bond distances and bond angles of the $Ru_2(L)_4$ framework of **1** also fall within the range of values observed for previously characterized (3,1) and (4,0) $Ru_2(L)_4$Cl complexes with similar types of bridging ligands,[13] and overall, the fact that the Me group is located on the pyridyl rather than the anilino site of the ap ligand does not yield significant structural changes in the $Ru_2(L)_4$ framework (see Table 2). The only exception is the average N−Ru−Ru−N torsion angle, which is 13.9° for **1** as compared to 21.6 ° for Ru_2(2-Meap)$_4$Cl and 17.0−19.7° for the (3,1) isomers of $Ru_2(L)_4$Cl where L = 2-Fap, 2,6-F_2ap, or 2,4,6-F_3ap.[13]

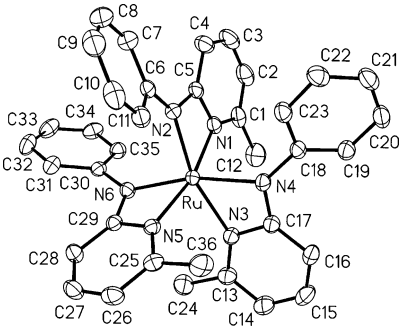

Figure 2. Molecular structure of Ru(ap-6-Me)$_3$, **2**. H atoms have been omitted for clarity.

Table 3. Selected Bond Lengths (Å) and Bond Angles (deg) for **2**

	Bond Lengths (Å)		
Ru−N1	2.0559(15)	Ru−N2	2.0358(15)
Ru−N3	2.1045(16)	Ru−N4	2.0886(15)
Ru−N5	2.0908(15)	Ru−N6	2.0383(15)
	Bond Angles (deg)		
N1−Ru−N2	64.00(6)	N1−Ru−N4	86.65(6)
N3−Ru−N4	62.80(6)	N2−Ru−N6	90.81(6)
N5−Ru−N6	63.68(6)	N3−Ru−N5	84.65(6)

Structural Characterization of 2. An ORTEP diagram of **2** is illustrated in Figure 2, while selected bond lengths and bond angles are listed in Table 3. Figure 2 shows that each ap ligand is coordinated to the ruthenium atom through the pyridyl and the anilino nitrogen atoms, giving a four-membered ring with an average bite angle of 63° (see Table 3). The ruthenium atom exhibits an N_6 coordination environment with a distorted octahedral geometry. The relative position of the pyridyl and the anilino nitrogen atoms indicates that the compound adopts a so-called meridional stereochemistry, which is quite common to other structurally characterized tris-chelate ruthenium(III) derivatives.[30] The Ru−N_{py} (N_{py} = pyridyl nitrogen) bond lengths are slightly elongated as compared to those in neutral Ru(III) complexes with the same type of structure,[30] and **2** exhibits one short Ru−N_{py} bond and two long Ru−N_{py} bonds as compared to two short and one long Ru−N_{py} bond for Ru(L-OCH_3)$_3$ where L is an amide anion.[30] The average Ru−N_a (N_a = anilino nitrogen) bond length in **2** is also 0.1 Å longer than the average Ru−N_a bond distance in **1**, but an opposite trend is observed for the average Ru−N_{py} bond length which is 0.1 Å shorter in **2**.

ESR Spectra. The ESR spectrum of frozen **2** is illustrated in Figure 3. The spectrum exhibits a typical rhombic signal with a g tensor characterized by three well-defined components at 2.42, 2.28, and 1.88. This clearly indicates that **2** contains a low-spin Ru(III) ion, and this assignment was further confirmed by the fact that the compound possess only one unpaired electron, as indicated by the magnetic moment of 1.75 μ_B at room temperature (see Experimental Section). No ESR signal was observed for **1**, consistent with the presence of three unpaired electrons[1,3,4,13,37−40] and a magnetic moment of 4.19 μ_B at room temperature (see Experimental Section).

Redox Properties of 2. Figure 4 illustrates cyclic voltammograms of **2** in PhCN and CH_2Cl_2, both of which contain

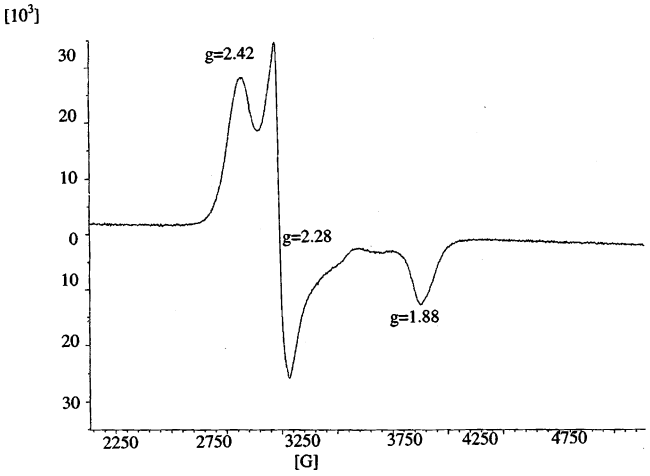

Figure 3. ESR spectrum of **2** in CH_2Cl_2, 0.2 M TBAP at 77 K.

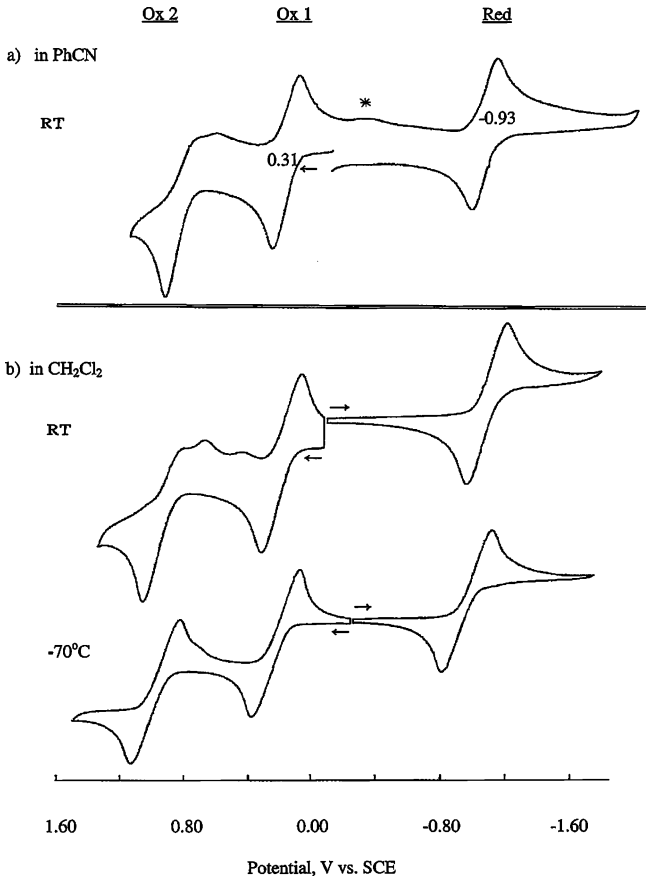

Figure 4. Cyclic voltammograms of **2** in (a) PhCN, 0.1 M TBAP at room temperature and (b) CH_2Cl_2, 0.1 M TBAP at room temperature and −70 °C. Scan rate = 0.1 V/s. The asterisk indicates a decomposition product generated upon scanning the potential beyond the second oxidation of the compound.

0.1 M TBAP as supporting electrolyte. The PhCN data was obtained at room temperature, while measurements in CH_2Cl_2 were carried out at room temperature and −70 °C.

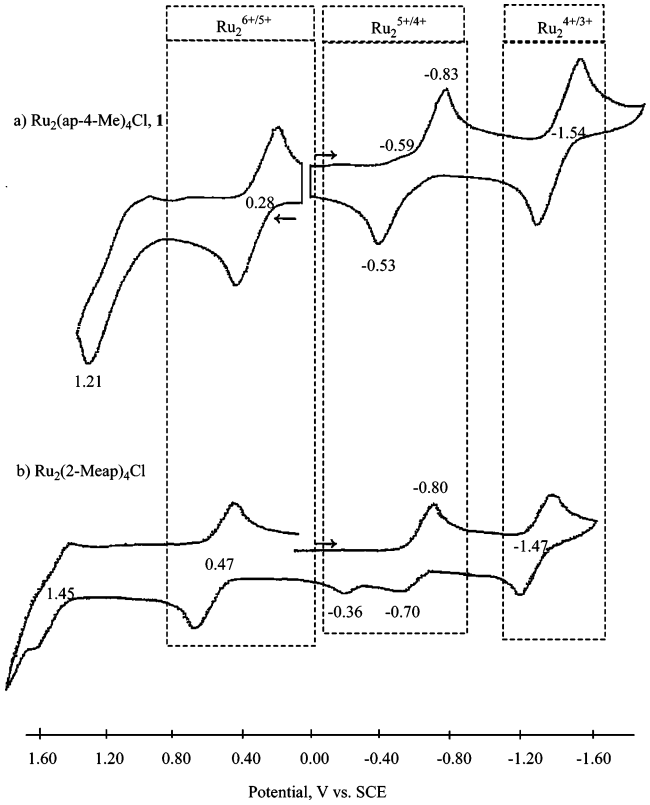

Figure 5. Cyclic voltammogram of (a) **1** and (b) $Ru_2(2\text{-Meap})_4Cl$ in PhCN, 0.1 M TBAP. Scan rate = 0.1 V/s. The voltammograms for $Ru_2(2\text{-Meap})_4Cl$ is reproduced from ref 3.

Scheme 1. Reduction Mechanism in PhCN, under N_2

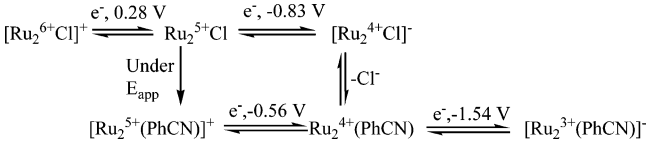

Under all conditions, Ru(ap-6-Me)$_3$ is characterized by only a single reversible reduction up to the negative potential limit of the solvents (about −1.85 V) and two oxidations, the second of which is irreversible at room temperature (RT) in both PhCN and CH_2Cl_2 but reversible at −70 °C in CH_2Cl_2.

Only metal-centered processes are known for reduction of monoruthenium(III) complexes with a structure similar to that of **2**.[28,30−33] A Ru(III)/Ru(II) reduction couple is therefore proposed for the first RT reduction of **2** at $E_{1/2}$ = −0.93 V in PhCN or CH_2Cl_2, and this assignment is also consistent with the UV−visible spectrum of the electro-reduced product in a thin-layer cell (see next section).

The first oxidation of previously examined Ru(L)$_3$ complexes with non-ap-type ligands has been reported as involving either the Ru^{III} metal ion[28,30,31,33] or the anionic bridging ligand.[32] The first oxidation of **2** in PhCN, 0.1 M TBAP is a reversible process (see Figure 4a), and the $E_{1/2}$ value of 0.31 V in both solvents suggests a metal-centered reaction, i.e., Ru(III)/Ru(IV). The second RT oxidation of **2** occurs at a more positive potential of E_p = 1.00 V in PhCN and E_p = 1.10 V in CH_2Cl_2 at a scan rate of 0.1 V/s. This reaction becomes reversible at −70 °C in CH_2Cl_2, 0.1 M TBAP where $E_{1/2}$ = 1.01 V (see Figure 4b). This oxidation

(37) Li, Y.; Han, B.; Kadish, K. M.; Bear, J. L. *Inorg. Chem.* **1993**, *32*, 4175−4176.
(38) Cotton, F. A.; Torralba, R. C. *Inorg. Chem.* **1991**, *30*, 2196−2207.
(39) Bear, J. L.; Han, B.; Huang, S. *J. Am. Chem. Soc.* **1993**, *115*, 1175−1177.
(40) Bear, J. L.; Li, Y.; Han, B.; Kadish, K. M. *Inorg. Chem.* **1996**, *35*, 1395−1398.

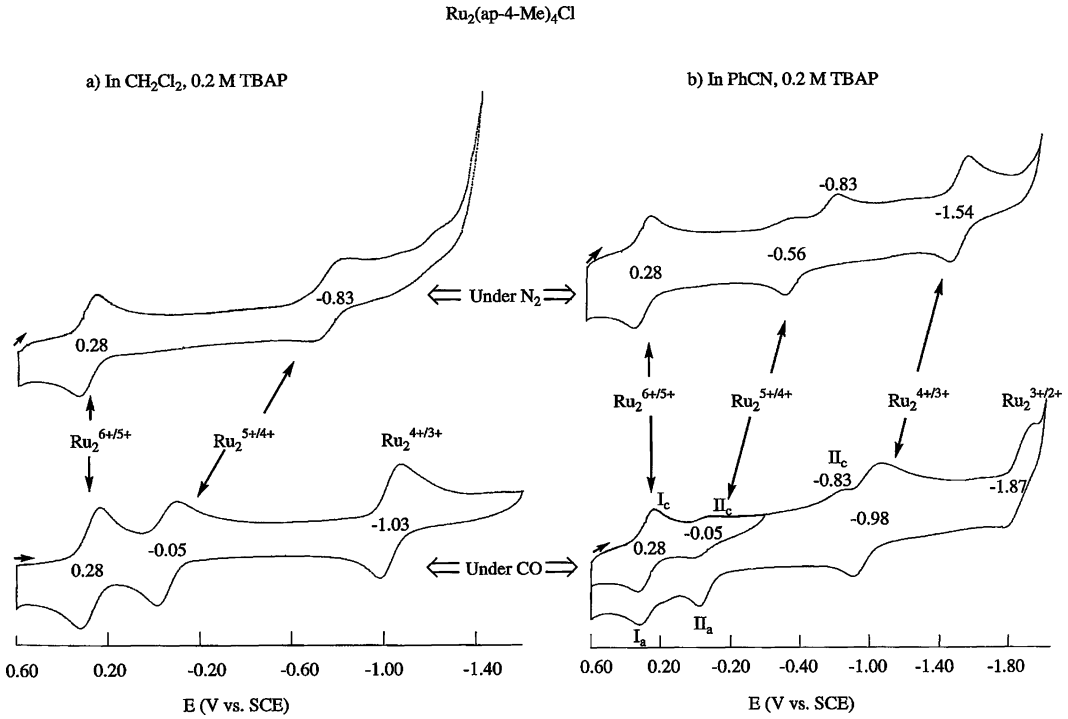

Figure 6. Cyclic voltammograms of **1** (a) in CH_2Cl_2 and (b) in PhCN, 0.2 M TBAP under an N_2 or CO atmosphere. Scan rate = 0.1 V/s.

is proposed to be ligand-centered, and the reversible $E_{1/2}$ value can be compared to an $E_p = 1.32$ V for oxidation of the free ligand H(ap-6-Me) under the same solution conditions at a scan rate of 0.1 V/s. A ligand-centered oxidation was also assigned to the second oxidation of $Ru^{III}(L)_3$ in CH_2Cl_2 where L = the N,S-bidentate ligand 2-(2-pyridyl)-benzenethiol.[33]

The potential separation between the metal- and the ligand-centered oxidations of the above 2-(2-pyridyl)benzenethiol $Ru^{III}(L)_3$ compound was reported to be 770 mV in CH_2Cl_2,[33] and this value is close to the measured 700 mV potential separation between the two reversible oxidations of **2** in CH_2Cl_2, 0.1 M TBAP at low temperature ($E_{1/2} = 0.31$ and 1.01 V). Although one cannot exclude the possibility of a Ru(IV)/Ru(V) couple for the second oxidation of **2**, this assignment is unlikely and more compounds of the same type must be synthesized and investigated to prove or disprove this point.

Electrochemistry of 1. Cyclic voltammograms of **1** and Ru_2(2-Meap)$_4$Cl in PhCN, 0.1 M TBAP are shown in Figure 5. The electrochemistry of the latter compound has been described in the literature.[11] Both diruthenium complexes (Figure 5) are reduced via two one-electron-transfer steps as opposed to a single one-electron-transfer step in the case of **2** (Figure 4). In addition, the first reduction of Ru_2(2-Meap)$_4$Cl, i.e., the $Ru_2^{5+/4+}$ process, is characterized by two, rather than one, reoxidation peaks which occur at $E_p = -0.70$ and -0.36 V vs SCE for a scan rate of 0.1 V/s (see Figure 5b).[11] The potential separation between E_{pc} for the first reduction of Ru_2(2-Meap)$_4$Cl (-0.80 V) and its reoxidation peak at $E_{pa} = -0.36$ V is 420 mV for a scan rate of 0.1 V/s, and this value can be compared to a 300 mV potential separation between E_{pc} for the first reduction of **1** (-0.83 V) and its reoxidation peak at $E_{pa} = -0.53$ V (see Figure 5a). This suggests a similar reduction mechanism for **1** and Ru_2(2-Meap)$_4$Cl, the related methyl-ap-substituted compound. However, in the case of **1**, a small reduction at $E_{pc} = -0.59$ V is also coupled to the reoxidation at $E_{pa} = -0.53$ V. These two peaks are attributed to the reversible conversion of $[Ru_2(ap\text{-}4\text{-}Me)_4(PhCN)]^+$ to $Ru_2(ap\text{-}4\text{-}Me)_4(PhCN)$, the former of which is generated under an applied potential, as shown in Scheme 1, where $E_{1/2} = -0.56$ V for this process.

The mechanism for oxidation of **1** and Ru_2(2-Meap)$_4$Cl are also similar in that they both involve $Ru_2^{5+/6+}$ and $Ru_2^{6+/7+}$ processes. However, as seen in Figure 5, the half-wave potentials for these oxidations are different from each other and seem to be more affected by the location of the methyl substituent on the bridging ligand than in the case of the reductions. Here, **1** is 190 mV easier to oxidize than Ru_2(2-Meap)$_4$Cl (0.28 vs 0.47 V).

Reactivity of 1 under CO. Figure 6a illustrates cyclic voltammograms of **1** in CH_2Cl_2, 0.2 M TBAP under N_2 and CO atmospheres. Two reversible redox reactions are observed under N_2 as compared to three under a CO atmosphere. The first oxidation of **1**, i.e., the $Ru_2^{6+/5+}$ couple at $E_{1/2} = 0.28$ V, is unaffected by the gas above the solution, while $E_{1/2}$ for the $Ru_2^{5+/4+}$ process shifts from -0.83 V under N_2 to -0.05 V under CO. A third redox couple, the $Ru_2^{4+/3+}$ process, is observed at $E_{1/2} = -1.03$ V under a CO atmosphere but not detected under N_2. A similar effect of CO binding was also observed for the electrochemistry of $Ru_2(dpf)_4Cl$ under the same solution conditions.[12]

Figure 6b illustrates cyclic voltammograms of the same compound, **1**, in PhCN, containing 0.2 M TBAP under an N_2 or CO atmosphere. Again, the first oxidation, the $Ru_2^{5+/6+}$ couple, is unaffected by the gas over the solution but the $Ru_2^{5+/4+}$ process in PhCN shifts positively in potential under a CO atmosphere. This reduction is also split into two distinct

Scheme 2. Reduction Mechanism in PhCN, under CO

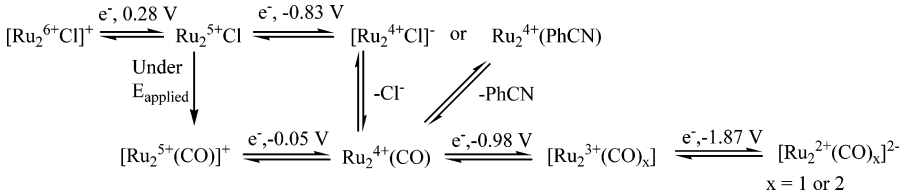

processes at $E_{1/2} = -0.05$ V and $E_p = -0.83$ V. The peak at $E_{1/2} = -0.05$ V in PhCN is assigned as a reduction of $[Ru_2(ap\text{-}4\text{-}Me)_4(CO)]^+$ to give $Ru_2(ap\text{-}4\text{-}Me)_4(CO)$ while the reduction at $E_p = -0.83$ V is assigned as a conversion of $Ru_2(ap\text{-}4\text{-}Me)_4Cl$ to $[Ru_2(ap\text{-}4\text{-}Me)_4(Cl)]^-$ or $Ru_2(ap\text{-}4\text{-}Me)_4(PhCN)$ followed by loss of Cl^- and/or PhCN and binding of CO to yield $Ru_2(ap\text{-}4\text{-}Me)_4(CO)$ as a final Ru_2^{4+} reduction product. The assignment of only a single CO molecule to the Ru_2^{4+} form of the compound is based on previous work with related compounds where only a single CO molecule is shown to coordinate to $Ru_2^{4+}(L)_4$.[12,15]

Additional electroreductions of **1** are also observed under a CO atmosphere and located at $E_{1/2} = -0.98$ and -1.87 V for the third and fourth processes, respectively. These electron-transfer reactions are attributed to the $Ru_2^{4+/3+}$ and $Ru_2^{3+/2+}$ redox couples on the basis of similar assignments made for related $Ru_2(L)_4Cl$ complexes under the same experimental conditions,[12,15] and the overall proposed electroreduction mechanism is shown in Scheme 2.

Reactivity of 1 in PhCN Solutions with Added CN^-. Figure 7 illustrates cyclic voltammograms of **1** in PhCN, 0.2 M TBAP before and after addition of TBACN. Four redox processes are observed when 1.0 equiv of TBACN is added to solution (Figure 7b), and based on earlier work[10] for $Ru_2(ap)_4Cl$, in the presence of CN^-, it can be concluded that the two peaks at $E_{1/2} = +0.39$ and -0.35 V involve the $Ru_2^{7+/6+}$ and $Ru_2^{6+/5+}$ couples of the bis-cyano complex, respectively. The reversible couple at $E_{1/2} = -0.79$ V is attributed to the $Ru_2^{5+/4+}$ process of **1**, and the irreversible peak at $E_{pc} = -1.24$ V is assigned to the $Ru_2^{5+/4+}$ reaction of the bis-cyano complex. When adding 2 equiv of TBACN to solution (Figure 7c), the currents for the process at -0.79 V diminish in intensity, which is consistent with **1** being consumed and a larger concentration of $Ru_2(ap\text{-}4\text{-}Me)_4(CN)_2$ being formed in solution. Here the major redox processes of the bis-CN complex occur at $E_p = 0.47$ V, $E_{1/2} = -0.35$ V, and $E_{1/2} = -1.28$ V. The remaining couples at $E_{1/2} = -0.69$ and -0.79 V are assigned to reduction of $Ru_2(L)_4$-CN and $Ru_2(L)_4Cl$, respectively.

UV−Vis Spectroelectrochemistry. Oxidation. Figure 8a and b illustrates the time-dependent spectral changes which occur upon the first oxidation of **1** in PhCN, 0.2 M TBAP and **2** in CH_2Cl_2, 0.2 M TBAP. There is a formation of a new band at 845 nm for singly oxidized $Ru(ap\text{-}6\text{-}Me)_3$ (Figure 8b). The appearance of a broad band centered at 884 nm and the loss of the 739 nm are the major time-dependent spectral changes observed during the Ru_2^{5+}/Ru_2^{6+} process of $Ru_2(ap\text{-}4\text{-}Me)_4Cl$ (Figure 8a). Similar spectral features are also observed after the one-electron oxidation of $Ru_2(L)_4Cl$ where L is a ligand with substituents on the anilino part of the ap ligand, i.e., Fap, F_3ap, or F_5ap.[11,13] It has been proposed[13] that the one-electron oxidation of $Ru_2(L)_4Cl$ where L = ap, Fap, F_3ap, or F_5ap involves an abstraction of the electron from the δ^* orbital; the UV−vis spectrum of singly oxidized $Ru_2(ap\text{-}4\text{-}Me)_4Cl$ is also consistent with this assignment.

Reduction. The UV−visible spectral changes during reduction of **1** and **2** are shown in Figure 8c and d. The first reduction of $Ru_2(ap\text{-}4\text{-}Me)_4Cl$ leads to disappearance of the 739 nm band for the neutral compound concomitant with an increase in intensity of a band at 475 nm (Figure 8c). A similar trend in the spectral changes is observed upon reduction of **2** where the 750 nm band vanishes upon

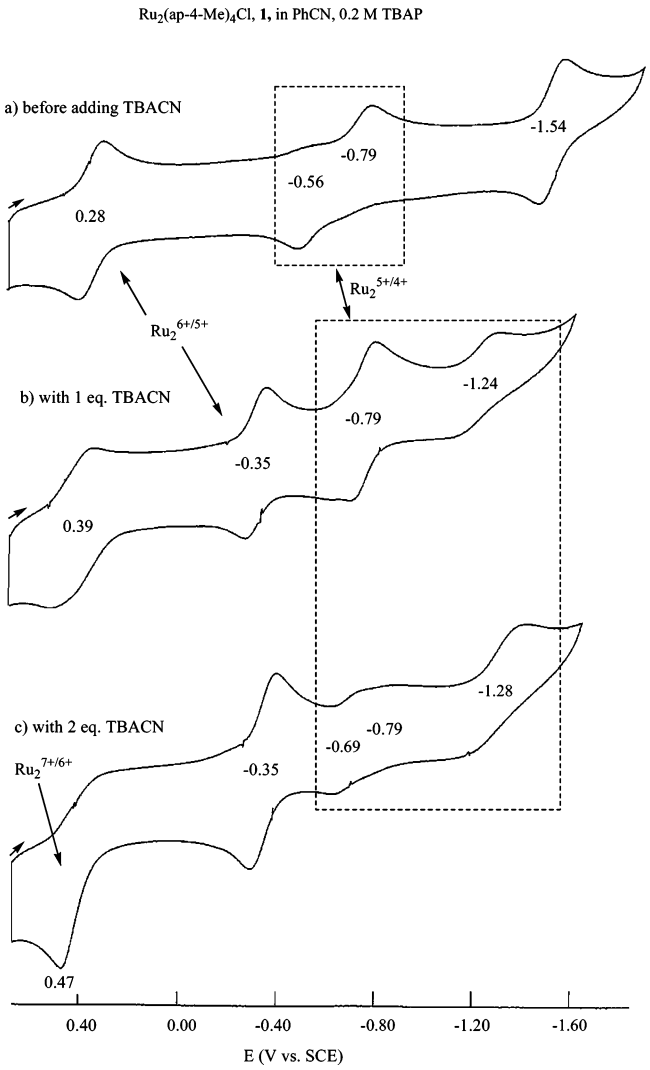

Figure 7. Cyclic voltammograms of **1** in PhCN, 0.2 M TBAP (a) before adding TBACN, (b) with 1 equiv of TBACN, and (c) with 2 equiv of TBACN. Scan rate = 0.1 V/s.

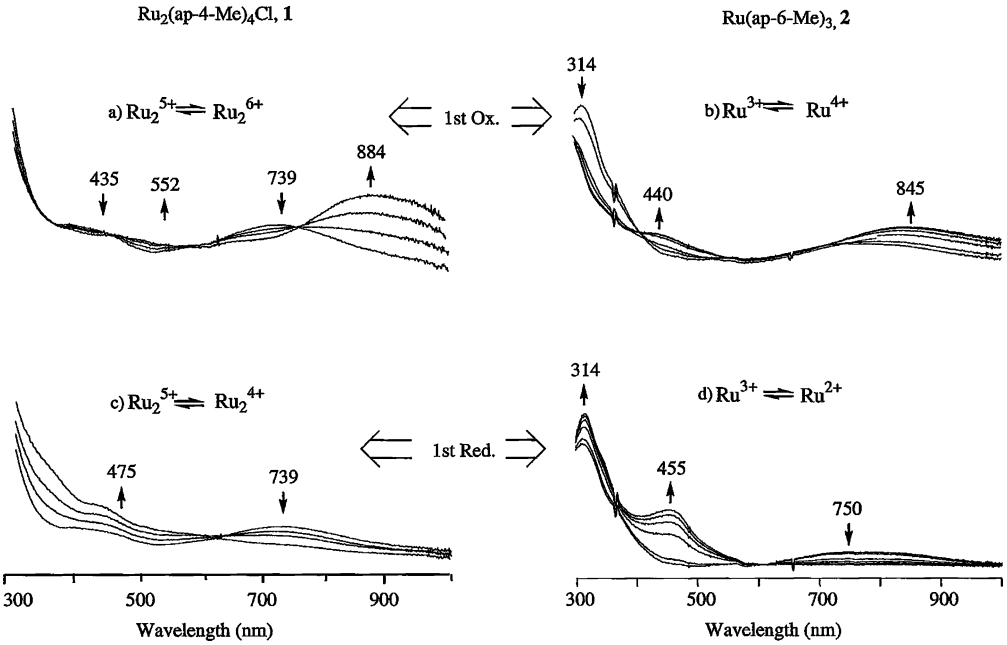

Figure 8. UV−vis spectral changes upon the first oxidation of (a) **1** in PhCN, 0.1 M TBAP and (b) **2** in CH_2Cl_2, 0.2 M TBAP and upon the first reduction of (c) **1** in PhCN, 0.1 M TBAP and (d) **2** in CH_2Cl_2, 0.2 M TBAP.

reduction and a new higher-intensity band grows in at 455 nm (Figure 8d).

Neutral **2** exhibits two bands in CH_2Cl_2, 0.2 M TBAP; one is intense and located at $\lambda_{max} = 314$ nm, and the other is weak and located at $\lambda_{max} = 750$ nm (see Figure 8d). The band at 750 nm is assigned as a LMCT transition[28−33] which is most likely ap (π) → d, while the intense high-energy band is proposed to involve an intraligand $\pi \rightarrow \pi^*$ transition on the basis of what has been assigned to intense bands between 330 and 340 nm in the case of other similar Ru(III) complexes.[28,30,33] A 455 nm band is seen upon reduction of **2** and is proposed to involve a MLCT transition of the type d → π^* (ap-6-Me) on the basis of similar assignments of absorption bands for Ru(II) complexes[29,31] with a geometry similar to that of $Ru(ap\text{-}6\text{-}Me)_3$.

Summary. In summary, we report in the present paper the first examples of ruthenium complexes containing 2-anilinopyridinate anionic bridging ligands substituted on the pyridyl rather than anilino sites of the molecule and show that a clear difference is seen in the nature of the ruthenium complex formed in a reaction between this type of ligand and $Ru_2(O_2CCH_3)_4Cl$. More specifically, the reaction with an ap ligand where the methyl substituent is at the para position of the pyridyl group yields exclusively a diruthenium(III,II) complex, i.e., (3,1) $Ru_2(ap\text{-}4\text{-}Me)_4Cl$, while the reaction with an ap ligand where the methyl substituent is at the ortho position of the pyridyl group yields exclusively a monoruthenium complex, i.e., $Ru(ap\text{-}6\text{-}Me)_3$. The fact that the CH_3 substituent is on the pyridyl rather than the anilino group of the ap ligand in $Ru_2(ap\text{-}4\text{-}Me)_4Cl$ does not affect significantly the structural framework of the compound, but it does induce a greater lability of the Cl^- axial ligand which brings about changes in the electrochemical behavior and redox reactivity of this compound toward CO as compared to what was earlier observed for $Ru_2(2\text{-}Meap)_4Cl$ and related compounds. The strong binding of CO to the Ru_2^{4+} complex has possible ramifications in the development of CO sensors and will be explored in further studies.

Acknowledgment. The support of the Robert A. Welch Foundation (J.L.B., Grant No. E-918; K.M.K., Grant No. E-680) is gratefully acknowledged. We thank Dr. J. D. Korp for carrying out the X-ray analyses.

Supporting Information Available: X-ray crystallographic files, in CIF format, for compounds $Ru_2(ap\text{-}4\text{-}Me)_4Cl$, **1**, and $Ru(ap\text{-}6\text{-}Me)_3$, **2**. This material is available free of charge via the Internet at http://pubs.acs.org.

IC060267K